Cardiovascular Research (2013) **97**, 676–685
doi:10.1093/cvr/cvs424

Pressure-overload-induced heart failure induces a selective reduction in glucose oxidation at physiological afterload

Pavel Zhabyeyev[1], Manoj Gandhi[2], Jun Mori[1,2,3,4,5], Ratnadeep Basu[3,4], Zamaneh Kassiri[3,4], Alexander Clanachan[2], Gary D. Lopaschuk[2,4,5]*, and Gavin Y. Oudit[1,3,4]*

[1]Division of Cardiology, Department of Medicine, University of Alberta, 8440 112 Street NW, Edmonton, AB, Canada T6G 2B7; [2]Department of Pharmacology, University of Alberta, Edmonton, Canada; [3]Department of Physiology University of Alberta, Edmonton, Canada; [4]Mazankowski Alberta Heart Institute, University of Alberta, Edmonton, Canada; and [5]Department of Pediatrics, 423 Heritage Medical Research Center, University of Alberta, Edmonton, AB, Canada T6G 2S2

Received 9 August 2012; revised 16 November 2012; accepted 17 December 2012; online publish-ahead-of-print 19 December 2012

Time for primary review: 25 days

Aims Development of heart failure is known to be associated with changes in energy substrate metabolism. Information on the changes in energy substrate metabolism that occur in heart failure is limited and results vary depending on the methods employed. Our aim is to characterize the changes in energy substrate metabolism associated with pressure overload and ischaemia–reperfusion (I/R) injury.

Methods and results We used transverse aortic constriction (TAC) in mice to induce pressure overload-induced heart failure. Metabolic rates were measured in isolated working hearts perfused at physiological afterload (80 mmHg) using ^{3}H- or ^{14}C-labelled substrates. As a result of pressure-overload injury, murine hearts exhibited: (i) hypertrophy, systolic, and diastolic dysfunctions; (ii) reduction in LV work, (iii) reduced rates of glucose and lactate oxidations, with no change in glycolysis or fatty acid oxidation and a small decrease in triacylglycerol oxidation, and (iv) increased phosphorylation of AMPK and a reduction in malonyl-CoA levels. Sham hearts produced more acetyl CoA from carbohydrates than from fats, whereas TAC hearts showed a reverse trend. I/R in sham group produced a metabolic switch analogous to the TAC-induced shift to fatty acid oxidation, whereas I/R in TAC hearts greatly exacerbated the existing imbalance, and was associated with a poorer recovery during reperfusion.

Conclusions Pressure overload-induced heart failure and I/R shift the preference of substrate oxidation from glucose and lactate to fatty acid due to a selective reduction in carbohydrate oxidation. Normalizing the balance between metabolic substrate utilization may alleviate pressure-overload-induced heart failure and ischaemia.

Keywords Pressure overload • Heart failure • Ischaemia–reperfusion • Energy metabolism

1. Introduction

Coronary artery disease and hypertension are prevailing causes of heart failure.[1,2] Metabolic perturbations in the heart that occur as a result of coronary artery disease and/or hypertension can play a key role in the pathogenesis of heart failure.[3,4] Other important mechanisms involved in the development of pathological hypertrophy and heart failure include abnormal signal transduction[5], mitochondrial dysfunction[3], and disrupted intracellular Ca^{2+} handling.[6] Most of these mechanisms affect utilization of energy substrates, which are required to generate ATP primarily for contraction. As heart failure progresses, cardiac energetic status (as measured by ATP and phosphocreatine content) is altered considerably.[3,7–9] However, specific details about the particular energy-generating pathways that underlie these reductions in high-energy phosphate levels are less clear. In human heart failure, there is a reversal to the foetal energy metabolic profile, resulting in a shift from fatty acid utilization towards glucose utilization.[3,10–12] The available data from animal models of heart failure are in general agreement with the findings in human heart failure. For example, *in vivo* measurements showed increased

* Corresponding author. Tel: +1 780 492 2170 (G.D.L.), +1 780 407 8569 (G.Y.O.); fax: +1 780 407 6452 (G.D.L.), +1 780 407 6452 (G.Y.O.), Email: glopasch@ualberta.ca (G.D.L.), gavin.oudit@ualberta.ca, (G.Y.O.)

glucose oxidation and decreased fatty acid oxidation in canine pacing-induced heart failure.[13] Similarly, *ex vivo* and *in vivo* metabolic rates in the pressure-overloaded rat and the spontaneously hypertensive rat (SHR) model showed early and substantial decrease in fatty acid oxidation with a relatively greater reliance on glucose oxidation.[14–16]

Murine models of heart failure are of considerable utility because of the multitude of transgenic and knockout strains available. This variety of gene-targeted murine models has the potential to provide considerable insight into the mechanism and the development of new therapies for heart failure. Emerging data suggest that cardiac metabolism is altered in murine models of heart disease.[17,18] In this study, we sought to characterize: (i) changes in energy substrate metabolism associated with pressure overload-induced heart failure and (ii) possible alterations in related regulatory pathways that may govern these changes. To describe metabolic alterations due to pressure overload in wild-type C57Bl/6 mice, we utilized an isolated working heart preparation, in which hearts were perfused at physiological preload (11.5 mmHg) and afterload (80 mmHg), and we also investigated how pressure-overloaded hearts respond to ischaemia–reperfusion (I/R) injury.

2. Methods

See Supplementary material online, Methods for detailed methodology.

2.1 Experimental animals

C57/Bl6 male mice ($n = 54$) weighing 27.5 ± 0.3 g were subjected to a transverse aortic constriction (TAC) or a sham procedure and, 6 weeks later, were subjected to an *ex-vivo* aerobic or I/R protocol (described below). All animals received care according to the standards of the Canadian Council of Animal Care, and all procedures were approved by the University of Alberta Health Sciences Animal Welfare Committee. All procedures were compliant with the Guide for the Care and Use of Laboratory Animals published by the US National Institutes of Health (NIH Publication, 8th edition, 2011; University of Alberta assurance number: A5070-01).

2.2 Pressure overload

Young (8- to 9-week-old) male mice were subjected to pressure overload as previously described.[19,20] Briefly, mice were anaesthetized with 1.5–2% isoflurane/oxygen and the surgical plane of anaesthesia was monitored by the lack of response to toe-pinching. The aortic arch was accessed via a left thoracotomy, and the thoracic aorta at the arch was surgically constricted against a 27-gauge needle to generate a trans-stenotic pressure gradient of 50–60 mmHg. The sham animals underwent the same procedure without aortic banding. Animals were studied at 5–6 weeks following the TAC or sham operations.

2.3 Echocardiography and tissue Doppler imaging

Mice were anaesthetized with 1% isofluorane/oxygen administered through inhalation. Transthoracic echocardiography and tissue Doppler imaging were performed non-invasively to assess systolic and diastolic function, as described previously, using a Vevo 770 high-resolution imaging system equipped with a 30-MHz transducer (RMV-707B; VisualSonics).[21]

2.4 Isolated working heart perfusions

Hearts were excised from mice after induction of anaesthesia with sodium pentobarbital (400 mg/kg, i.p.) and administration of heparin (100 units, i.p.), and the aorta and left atrium were rapidly cannulated, as described previously.[22,23] Hearts were initially perfused at an 11.5 mmHg left atrial (LA) preload, and a 50 mmHg aortic afterload. Within 3–5 min the aortic afterload was increased and maintained at 80 mmHg. The hearts were subjected to either aerobic perfusion for 45 min or to an I/R protocol where hearts were subjected to 45 min of aerobic perfusion, followed by 15 min of global ischaemia (37°C) and 30 min of aerobic reperfusion.

2.5 Measurement of mechanical function *ex vivo*

Isolated working heart perfusions were performed at atrial preload of 11.5 mmHg and a physiological aortic afterload of 80 mmHg. Hearts were paced at 380 b.p.m. LV power was calculated [cardiac output (CO) × (systolic pressure – LA preload)] and expressed as J min^{-1} g^{-1} dry weight.

2.6 Measurement of rates of glycolysis, glucose oxidation, lactate oxidation, fatty acid oxidation, and endogenous triacylglycerol (TG) oxidation

Measurements of rates of glycolysis and glucose, lactate, and fatty acid oxidation were performed using ^{3}H and ^{14}C radiolabelled substrates. The rates of glycolysis and glucose oxidation were measured by using tracer amounts of D-[5-^{3}H]glucose and D-[^{14}C]glucose in the heart perfusate, respectively, and quantifying $^{3}H_2O$ and $^{14}CO_2$ production, as described previously.[22,23] Rates of lactate oxidation and palmitate oxidation (fatty acid oxidation) were measured using tracer amounts of [^{14}C]lactate and [9, 10-^{3}H]palmitic acid, respectively. The measurement of changes in the TG content and incorporation of [^{3}H]palmitate into TG was used to calculate the contribution of fatty acid derived from TG during the periods of aerobic perfusion and reperfusion. Total TG was measured at 0, 45, and 90 min. Incorporation of [^{3}H]palmitate was measured in hearts frozen at the end of 45 and 90 min. The total TG content *minus* labelled TG content was used to calculate the contribution of unlabelled TG to fatty acid oxidation (endogenous) over the 45 min aerobic perfusion period (baseline). Similarly, changes in endogenous TG content and radiolabelled TG content at the end of reperfusion were calculated (the difference between 45 and 90 min). Rates of acetyl CoA production generated from glucose oxidation, lactate oxidation, exogenous palmitate oxidation and endogenous TGs were calculated based on a value of two acetyl CoA produced for each molecule of glucose oxidized, one acetyl CoA for each molecule of lactate oxidized, and eight acetyl CoA for each molecule of fatty acid oxidize and expressed as μmol min^{-1} g^{-1} dry weight, as described previously.[24]

2.7 Assay for glycogen content and glucose uptake

Glycogen from frozen heart powder was extracted and hydrolyzed to glucose, as previously described.[25] The amount of glucose was measured using a Sigma glucose kit (Sigma-Aldrich). Aliquots from the above hydrolyzed glycogen were used to measure incorporation of [^{3}H/^{14}C]glucose into glycogen (glycogen synthesis). The rates of glucose uptake were calculated as the sum of rates of glycolysis and glycogen synthesis, and are expressed as μmol min^{-1} g^{-1} dry weight.

2.8 Immunoblot analysis

Immunoblot analyses were performed as described previously.[26] Frozen ventricular tissue was homogenized to extract protein. After quantification by a Bradford protein assay kit (Bio-Rad), protein samples were subjected to SDS–polyacrylamide gel electrophoresis and transferred onto a nitrocellulose membrane. Following the pretreatment, membranes were probed with the appropriate antibodies. Immunoblots were visualized using an enhanced chemiluminescence western blot detection kit

(Perkin Elmer) and quantified with Image J software (U.S. National Institutes of Health). Membrane fractionation was performed for GLUT-4 immunoblotting.

2.9 Determination of malonyl CoA levels

Malonyl CoA levels[26] and PCr/ATP ratio[27] were measured in homogenized ventricular tissue (previously frozen) by high-performance liquid chromatography.

2.10 Statistics

All values are expressed as the mean ± the standard error of the mean (SEM) for n independent observations. Levels of significance were tested using Student's t-test or by ANOVA and Bonferroni *post hoc* tests with selected pairs for multiple comparisons. Differences were judged to be significant when $P < 0.05$. Statistical calculations were performed using GraphPad InStat (v.3.01).

3. Results

3.1 Pressure-overload-induced pathological hypertrophy and systolic dysfunction

3.1.1 Echocardiographic analysis

In comparison with the sham group, TAC mice demonstrated increased left-ventricular (LV) wall thickness, LV dilation, and systolic and diastolic dysfunction (*Figure 1A–J*). A marked increase in posterior wall thickness signified hypertrophy (*Figure 1B*), and a noticeable increase in LV end-diastolic dimension (LVEDD) suggested LV dilation

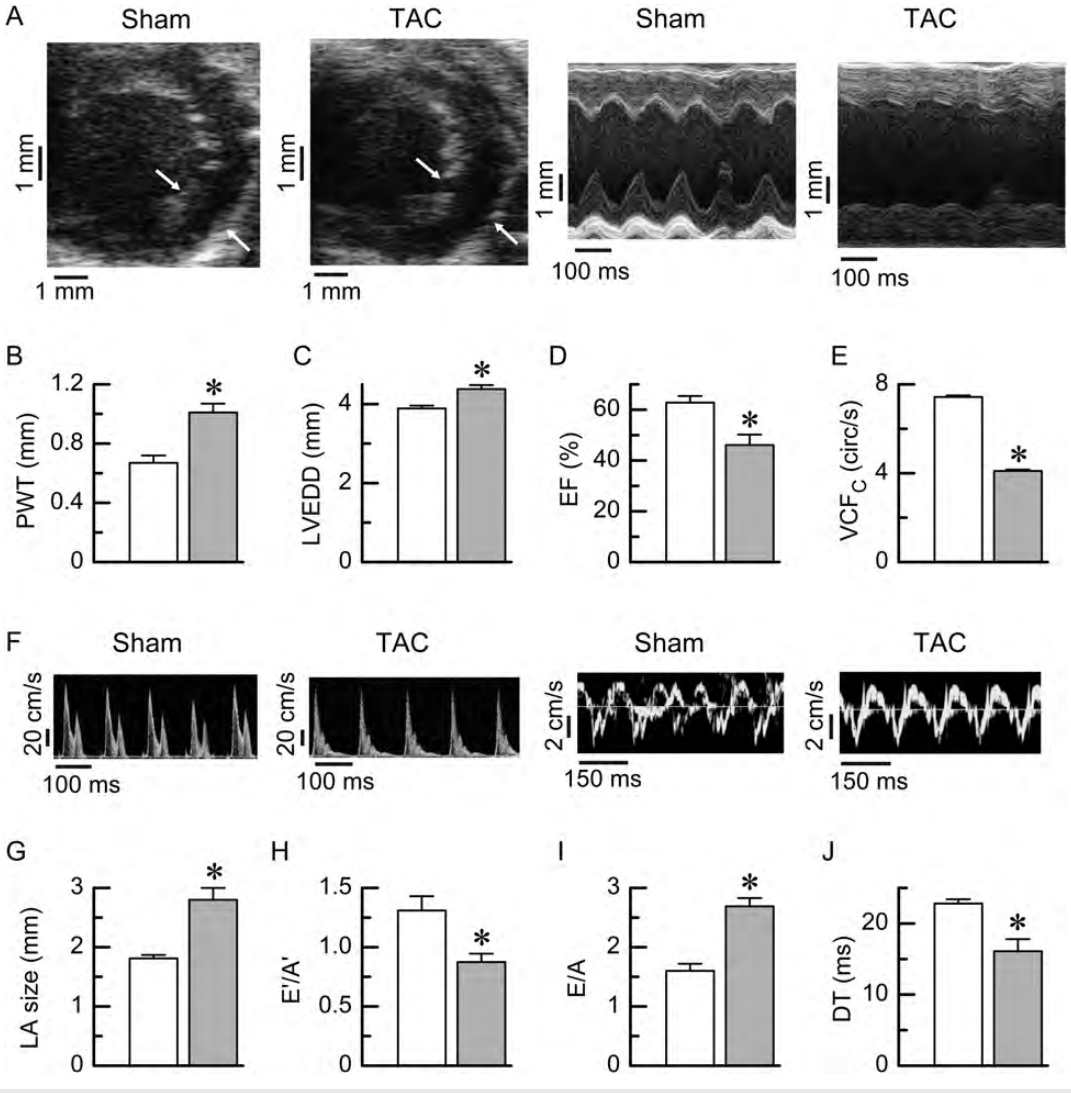

Figure 1 Echocardiographic characterization of cardiac systolic and diastolic function in mice subjected to TAC-induced pressure overload. (*A*) Representative echocardiographic images (B-mode—left and M-mode—right) from Sham and TAC mouse hearts. (*B–E*) Quantitative assessment of hypertrophy, dilation, and systolic function based on LV posterior wall thickness (PWT) (*B*), LV dilation (LVEDD—LV end-diastolic dimension) (*C*), ejection fraction (EF) (*D*), and velocity of circumferential shortening (VCF_C) (*E*). (*F*) Representative transmitral valvular flow profiles and tissue Doppler images from sham and TAC mouse hearts. (*G–J*) LA size (*G*) and quantitative assessment of diastolic function based on ratio of peak of E-wave (*E*) to early-diastolic tissue Doppler velocity (É) (E/É) (*H*), ratio of E-wave to A-wave (E/A) (*I*), and deceleration time (DT) (*J*). $n = 6$; white bars (sham group) and $n = 8$; grey bars (TAC group). *$P < 0.05$ compared with sham group.

(*Figure 1C*). Significant decreases in ejection fraction (EF) (*Figure 1D*) and velocity of circumferential shortening (VCF_C) in the TAC hearts compared with the sham hearts (*Figure 1E*) indicated systolic dysfunction. To assess diastolic function, mitral and tissue Doppler measurements and LA size were evaluated. Representative examples of transmitral flow and tissue Doppler are shown in *Figure 1F*. Pressure-overload changes in diastolic function revealed increased LA size, reduced E′/A′ ratio, increased E/A ratio, and shortened deceleration time in the TAC hearts (*Figure 1G–J*). These results show clear evidence of LV hypertrophy and systolic and diastolic dysfunction in response to TAC-induced pressure-overload.

3.1.2 Isolated working heart function

Heart weight (dry) was significantly higher (+71%) in the TAC group confirming pressure-overload hypertrophy (*Figure 2A* and *B*). Peak systolic pressure was significantly lower in TAC hearts compared with sham hearts (*Figure 2C*), whereas end-diastolic pressure was similar resulting in reduced developed pressure (DevP) in aortas of the TAC hearts (*Figure 2C* and *D*). Since hydrodynamic resistance is nearly constant in the working heart perfusion system, decreases in DevP invariably result in a decreased flow. All flow parameters were significantly reduced in the TAC hearts compared with sham hearts. Coronary flow (CF), aortic flow (AF), and CO decreased by 39, 69, and 58%, respectively (*Figure 2E* and *F*).

3.2 Pressure-overload-induced reduction in glucose and lactate oxidation

Metabolic rates of glucose, lactate, palmitate, and triacylglycerol oxidation were evaluated in the sham and TAC hearts. These measurements were done in pairs: glycolysis (^3H) with glucose oxidation (^{14}C), palmitate oxidation (^3H) with lactate oxidation (^{14}C), and TG was measured separately. Glucose metabolism was suppressed overall in hearts from TAC mice: rates of glucose oxidation decreased by 66% while rates of glycolysis trended to be lower (−28%, $P = 0.07$) (*Figure 3A*). Similarly, the rate of lactate oxidation was significantly lower (by 33%) whereas the rate of palmitate oxidation was unchanged (*Figure 3B*). The TG content decreased between 0 and 45 min of perfusion time (*Figure 3C*) and derived the rate of TG oxidation was lower in the TAC hearts (*Figure 3D*). These decreases in the energy substrate utilization in the TAC hearts resulted in an overall energy-compromised state of the hearts as illustrated by a decrease in the phosphocreatine–ATP ratio from 1.69 ± 0.04 ($n = 6$) in

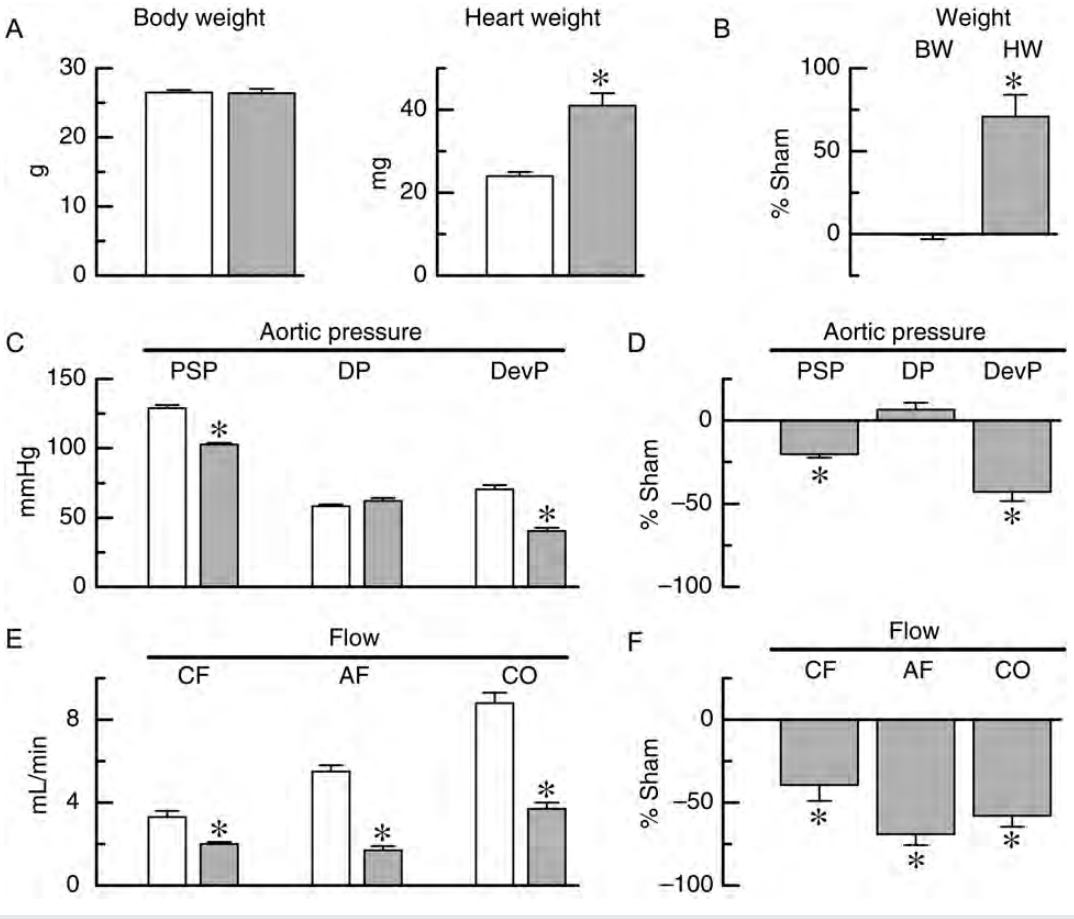

Figure 2 *Ex vivo* characterization of hypertrophy and hydrodynamic changes in mouse hearts in response to TAC-induced pressure overload. (*A* and *B*) Body weight, heart weight (dry) for sham and TAC hearts (*A*) and per cent changes in body weight and heart weight (*B*). (*C* and *D*) Aortic pressure parameters: peak systolic pressure (PSP), end-diastolic pressure (DP), and DevP in sham and TAC hearts, and per cent changes in these parameters (*D*). (*E* and *F*) Flow parameters: coronary flow (CF), arterial flow (AF), and cardiac output (CO) in sham and TAC hearts (*E*), and per cent changes in these parameters (*F*). $n = 12$; white bars (sham group) and $n = 12$; grey bars (TAC group). *$P < 0.05$ compared with sham group.

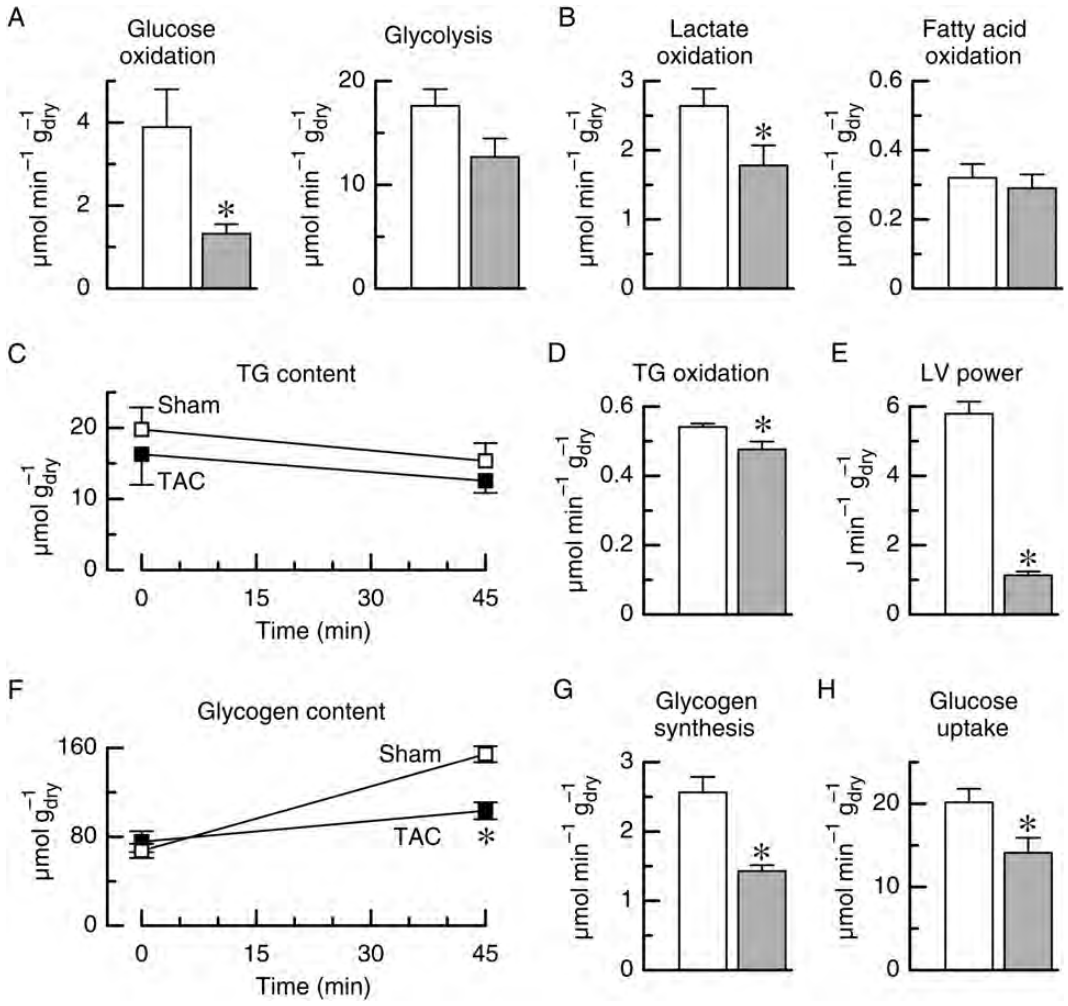

Figure 3 *Ex vivo* characterization of the changes in energy metabolic rates in mouse hearts in response to TAC-induced pressure-overload. (*A*) Glucose oxidation (left) and glycolysis (right) for Sham and TAC hearts. (*B*) Lactate oxidation (left) and fatty acid oxidation (right) for Sham and TAC hearts. (*C* and *D*) Triacylglycerol (TG) content (*C*) and TG oxidation (*D*) for Sham and TAC hearts. (*E*) LV power for Sham and TAC hearts. (*F*) Glycogen content at 0 and 45 min of the isolated working heart perfusions for Sham (open squares) and TAC (filled squares) hearts. (*G*) Glycogen synthesis in Sham and TAC hearts calculated from the data presented in (*F*). (*H*) Derived glucose uptake in Sham and TAC hearts calculated from (*A* and *G*). $n = 9$; white bars (Sham group) and $n = 9$; grey bars (TAC group). *$P < 0.05$ compared with the Sham group.

the sham hearts to 1.27 ± 0.11 ($n = 6$) in the TAC hearts ($P = 0.01$). The decreases were also accompanied by a reduction in LV power by 80% (*Figure 3E*). Decreases in the rates of glucose and lactate oxidation in hearts from the TAC mice raised the question as to whether the glycogen content and synthesis were affected by pressure-overload-induced heart disease. The glycogen content increased from 0 to 45 min in both sham and TAC hearts. However, in TAC hearts, the increase was smaller (*Figure 3F*) and the derived glycogen synthesis (*Figure 3G*) and glucose uptake (*Figure 3H*) were reduced.

3.3 Pressure-overload-induced changes in regulatory pathways

Given such marked changes in glucose metabolism and glycogen synthesis, we decided to assess possible alterations in: (i) the insulin pathway (Akt phosphorylation), (ii) the conversion of pyruvate to acetyl CoA [pyruvate dehydrogenase (PDH) phosphorylation and pyruvate dehydrogenase kinase isozyme 4 (PDK4) expression], (iii) the AMP-activated protein kinase (AMPK) pathway, (iv) acetyl CoA carboxylase (ACC) phosphorylation, malonyl CoA decarboxylase (MCD) expression, and malonyl CoA levels, (v) peroxisome proliferator-activated receptor gamma coactivator 1-α (PGC-1α) expression, and (vi) glucose transporter type 4 (GLUT4) levels. In the TAC hearts, Akt phosphorylation at both Thr308 and Ser473 residues was significantly down-regulated compared with sham hearts (by 58 and 54%, respectively) (*Figure 4A*). Neither PDH phosphorylation nor PDK4 expression was appreciably affected (*Figure 4B*). However, there were considerable alterations in the AMPK pathway. In TAC mice, myocardial AMPK phosphorylation increased by 150% (*Figure 4C*), which was accompanied by an increase in ACC phosphorylation by 120% (D). While there was a tendency for a decreased MCD expression (−23%, $P = 0.08$), malonyl CoA levels, which are controlled by ACC and MCD, were significantly lower (*Figure 4E*). PGC-1α expression levels were almost double in TAC hearts ($P = 0.04$) (*Figure 4F*).

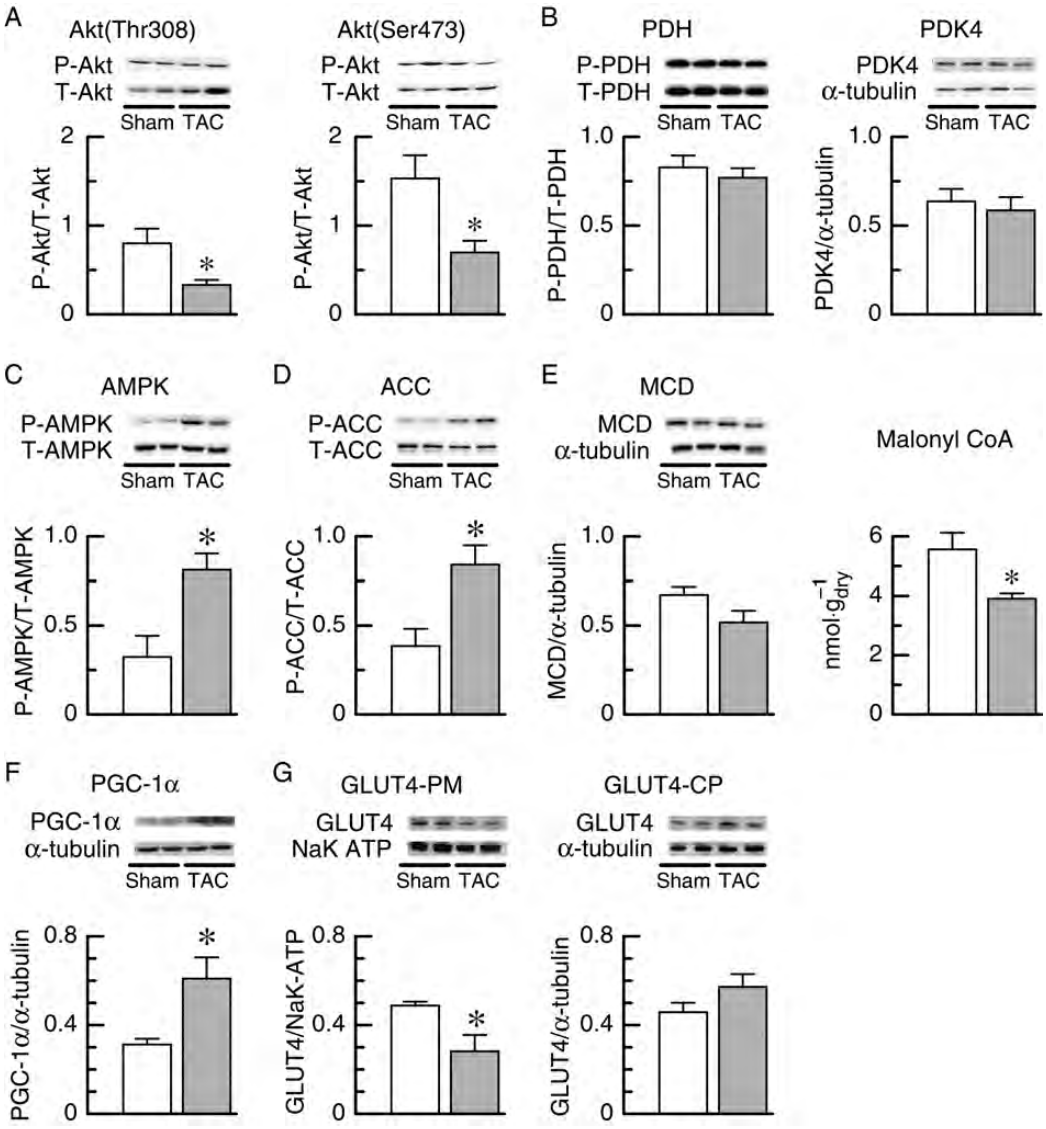

Figure 4 Characterization of pressure-overload induced changes in metabolic regulatory pathways. Changes in the phosphorylation levels of Akt (Thr308, left and Ser473, right) (*A*), and PDH (left) and expression levels of PDK4 (right) (*B*). Changes in phosphorylation levels of AMPK (*C*) and ACC (*D*) and changes in MCD (left) and malonyl CoA levels right) (*E*). Alterations in PGC-1α levels (*F*) and GLUT-4 levels in the plasma membrane (PM, left) and cytoplasm (CP, right) (*G*). PDH, pyruvate dehydrogenase; PDK4, pyruvate dehydrogenase; AMPK, AMP-activated protein kinase; ACC, acetyl CoA carboxylase; MCD, malonyl CoA decarboxylase, and PGC-1α, peroxisome proliferator-activated receptor γ co-activator 1-α. $n = 7$; white bars (sham group) and $n = 7$; grey bars (TAC group). *$P < 0.05$ compared with the Sham group.

Reduction in derived glucose uptake (*Figure 3H*) due to TAC was confirmed by the measurement of GLUT4 levels in the plasma membrane. The GLUT4 level in membrane (GLUT4-PM) of TAC hearts was decreased ($P = 0.04$) without changes in the cytoplasmic GLUT4 (GLUT4-CP) levels (*Figure 4G*).

3.4 I/R injury reduces glucose oxidation and increases TG oxidation

Co-existence of coronary artery disease in patients with pressure-overload-induced heart failure is a common clinical scenario. Indeed, heart failure is multifactorial with coronary artery disease and hypertension being the most common causes of heart failure.[1–3,28,29] To evaluate how pressure overload affects cardiac response to I/R, we subjected sham and TAC hearts to I/R protocol. While TAC hearts had baseline LV power (average LV power from 0 to 45 min) 80% lower than sham, following 15 min of global ischaemia, cardiac power in both groups substantially diminished (*Figure 5A*). To compare severity of I/R injury between groups, average time courses of LV power for both groups were normalized to respective baselines (*Figure 5B*). In the sham group, LV power initially recovered to 44% of baseline at 10 min post-reperfusion and then decreased to 36% at 30 min of the reperfusion period. In contrast, in the TAC hearts, cardiac power recovered to about 23% of pre-ischaemic level and stayed unchanged afterwards (*Figure 5B*). Lactate oxidation, palmitate oxidation, and glycolysis were unchanged by I/R. However, glucose oxidation rates showed a significant reduction in TAC hearts, coupled with an increased TG oxidation in both groups (*Figure 5C*).

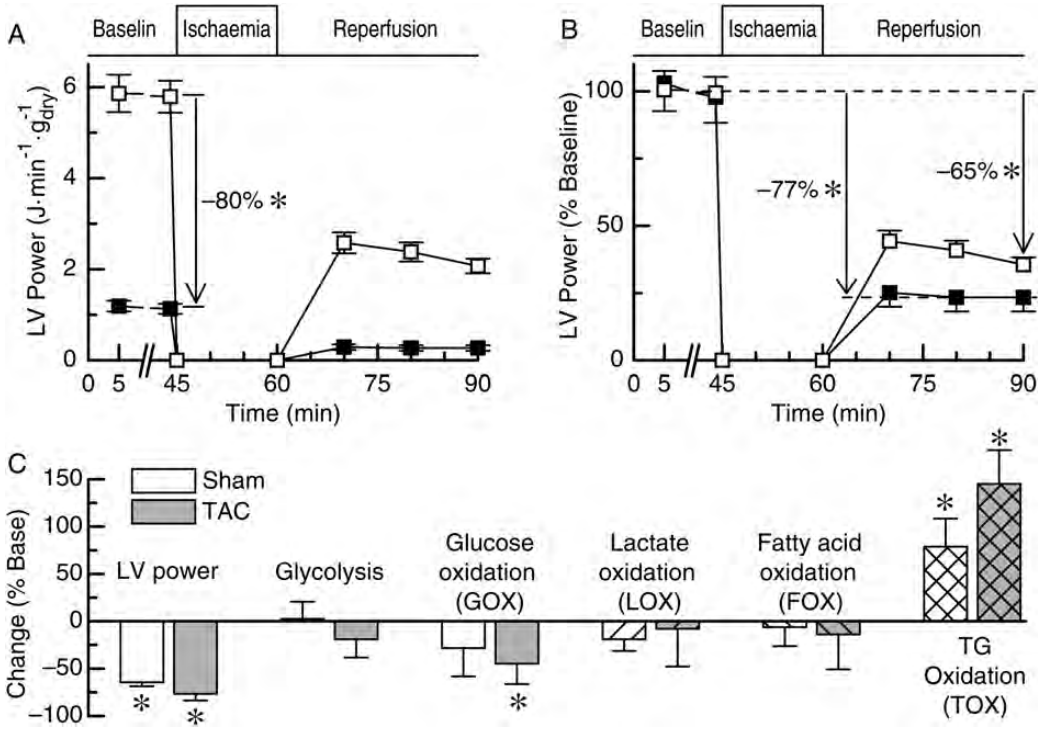

Figure 5 Response to I/R following pressure-overload induced heart disease. (*A*) Average time course of LV power for sham (open squares) and TAC (filled squares) hearts before and after ischaemia. (*B*) Time courses of LV power for Sham (open squares) and TAC (filled squares) hearts normalized to respective pre-ischaemic levels (baseline). (*C*) Summary of changes in LV power and various metabolic rates expressed as per cent change from pre-ischaemic level (baseline). Statistical comparisons are to pre-ischaemic levels of respective hearts. Sham group (white bars) and TAC group (grey bars); $n = 6–9$.

3.5 Changes in acetyl CoA production due to pressure overload and I/R injury

To gain further insight into the changes in oxidation rates of multiple substrates in the TAC hearts, we recalculated oxidation rates of all energy substrates to the equivalent amounts of acetyl CoA that is utilized in TCA cycle or *acetyl CoA production* (*Figure 6A*). Under baseline aerobic conditions, overall acetyl CoA production was decreased by 43% in TAC hearts compared with sham hearts. However, the overall reduction in the rate of acetyl CoA production (*Figures 6A*) was not in proportion with the decrease in LV power (*Figures 3*E and *5A*), which declined considerably more than the rate of the total acetyl-CoA production, suggesting a reduction in overall cardiac efficiency. Expressing cardiac efficiency as LV work per acetyl CoA (power divided by acetyl CoA production) reveals an overall reduction in cardiac efficiency of 66% for the TAC hearts compared with the sham hearts (*Figure 6B*, baseline). The decrease in acetyl CoA production was not uniform across energy substrates: glucose oxidation decreased, and lactate oxidation was reduced to a lesser extent (*Figure 6A*), whereas oxidation of fatty acids was largely unchanged (*Figure 6C*). As a result, sham hearts produced more acetyl CoA from glucose and lactate oxidation than from fatty acid and TG oxidation, whereas TAC hearts displayed the reverse situation. This demonstrated a shift in preferences for oxidative substrate from carbohydrates to fatty acids, which is clearly illustrated when acetyl CoA from each energy substrate is expressed as a per cent of the total acetyl CoA production (*Figure 6D*). In response to I/R, the total rate of acetyl CoA production was unchanged in sham hearts (*Figure 6A*), which in a setting of reduced LV power (*Figure 5B*) resulted in a lower cardiac efficiency. However, the composition of the acetyl CoA pool was altered, with a relative reduction in glucose oxidation and a significant increase in TG oxidation (*Figure 6C*). In contrast, I/R in the TAC hearts exacerbated these changes and increased the total rate of acetyl CoA production (*Figure 6A*) coupled with a reduction in cardiac power and compromised cardiac efficiency (*Figures 5B* and *6B*). The increase in the total rate of acetyl CoA production occurred due to an increase in TG oxidation (*Figure 6C* and *D*). These data show that pressure-overloaded heart failure is associated with reduced cardiac efficiency and increased susceptibility to I/R injury probably driven by the reduction in glucose oxidation and increase in TG oxidation.

4. Discussion

Pressure-overload, resulting from hypertension or aortic valvular stenosis, and coronary artery disease remain the most common causes of heart failure.[1,2,28,29] Metabolic defects can play a critical role in the initiation and progression of heart failure and metabolic modulators have been proposed as a potential therapy for heart failure.[3,4,30] As predicted, pressure-overload in our murine model resulted in LV hypertrophy and LV dilation, and both LV systolic and LV diastolic dysfunction. Importantly, energy metabolic profiling of the pressure-overloaded hearts revealed a clear shift from

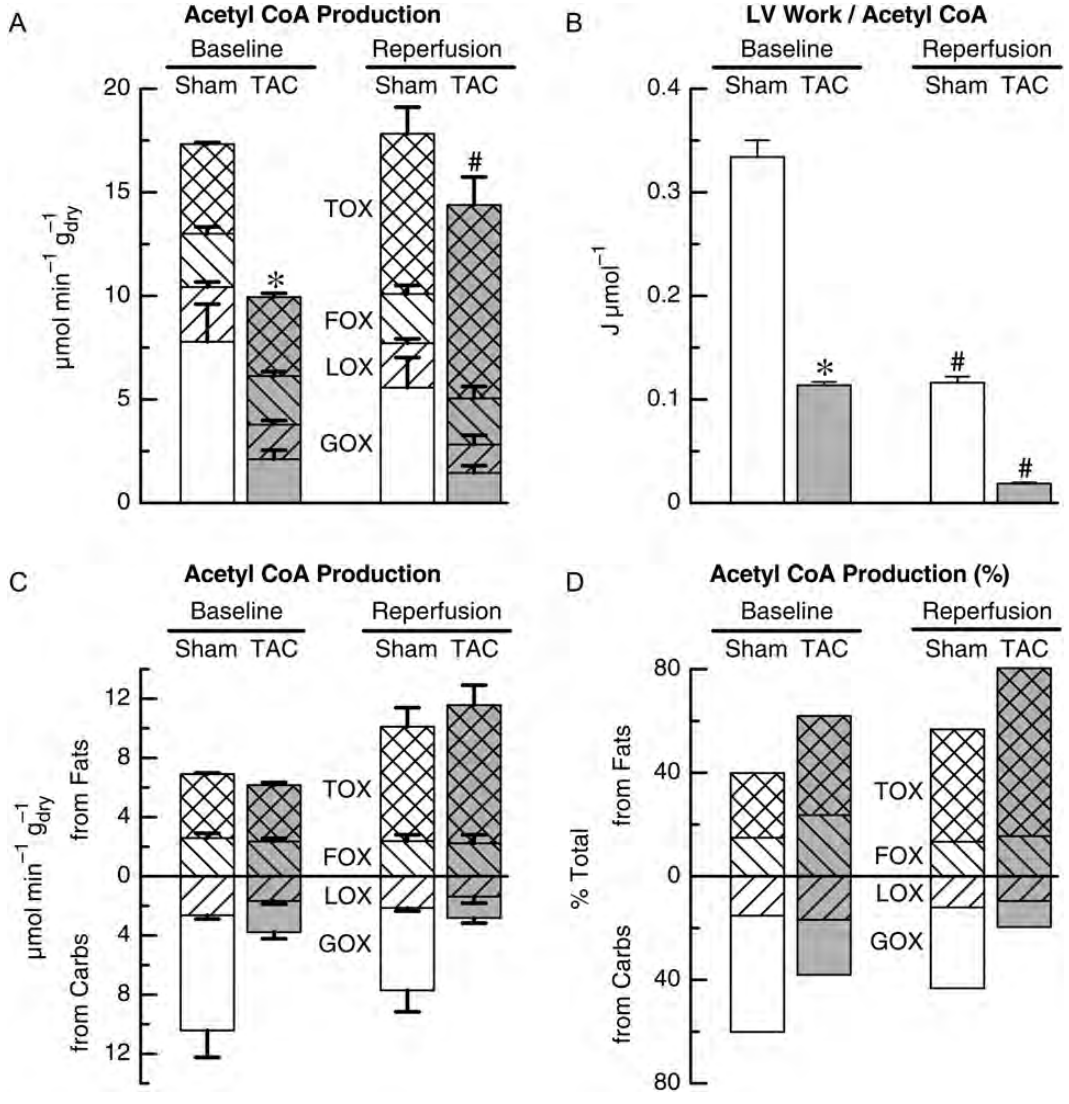

Figure 6 Acetyl CoA production under baseline and I/R conditions. (*A*) Calculated acetyl CoA production for glucose oxidation (GOX), lactate oxidation (LOX), fatty acid oxidation (FOX), and TG oxidation (TOX) before ischaemia (baseline) and after (reperfusion) for Sham and TAC hearts. (*B*) LV power adjusted by respective average of total acetyl CoA production. (*C*) Calculated acetyl CoA production grouped by carbohydrates (downward bars: glucose (GOX) and lactate (LOX) oxidation) and fatty acid oxidation (upward bars: fatty acid (FOX) and TG (TOX) oxidation). (*D*) Calculated acetyl CoA production grouped by carbohydrates and fatty acid oxidation expressed as per cent of total acetyl CoA production. $n = 9$; white bars (Sham group) and $n = 9$; grey bars (TAC group). $^{*}P < 0.05$ compared with the sham group; $^{\#}P < 0.05$ compared with baseline within respective group.

glucose to fatty acid and TG oxidation in hypertrophied mouse hearts. In response to I/R, pressure-overloaded hearts show an exacerbation of these energy metabolic changes, with a further lowering of carbohydrate oxidation, an increase in TG oxidation, and a reduced cardiac efficiency. Our findings appear to be discordant with recent findings which demonstrated enhanced glucose and reduced fatty acid oxidation in pressure-overload-induced heart disease.[17,18] However, although the recent study by Riehle *et al.*[17] only measured fatty acid oxidation in tissue homogenates following pressure overload hypertrophy in mice hearts, they did observe an actual increase in fatty acid oxidation rates in the wild-type hypertrophied mice hearts. Also of interest is that the study of Kolwicz *et al.*[18] demonstrated that in wild-type mice, pressure overload hypertrophy resulted in a much more dramatic increase in glycolysis than glucose oxidation in the heart. Combined, these data are consistent with our data showing a selective impairment in glucose oxidation compared with other metabolic pathways. The Kolwicz *et al.*[18] study also used hypertrophied mice heart with a very mild cardiac dysfunction. Comparison among studies is difficult, however, due to differences in animal models used with different degrees of heart disease, concentration of substrates, degree of afterload, and variation in the inclusion of insulin.

Two potential causes for the reduced rates of carbohydrate (glucose and lactate) oxidation in a setting of preserved fatty acid (palmitate) oxidation are: (i) insufficient availability of glucose or (ii) impaired conversion of pyruvate to acetyl CoA. Insufficient availability

of glucose can occur due to down-regulation of glucose transporters, which is consistent with reduced Akt phosphorylation and reduced levels of plasma-membrane GLUT4 in the TAC hearts. The decline in glycogen synthesis is also consistent with (i) down-regulation of the Akt signalling pathway and (ii) reduced glucose uptake due to reduced plasma-membrane GLUT4 levels; therefore, the reduced glycogen synthesis is likely reflective of an insulin-resistant state.[31] This result is in agreement with previous findings showing that lack of insulin signalling in the heart accelerates the transition to a more decompensated state during cardiac pressure-overload,[32] while over-expression of the GLUT1 transporter prevents pressure-overload-induced heart failure.[33] The conversion of pyruvate to acetyl CoA occurs via the PDH complex. Both phosphorylation of PDK4, the primary determinant of PDH activity, and expression of PDH were unaffected in the TAC hearts, suggesting that pyruvate conversion into acetyl CoA was not impaired. These molecular changes are clearly distinct from agonist-mediated hypertrophy and diastolic dysfunction in which glucose oxidation is also dramatically lowered, but with increased PDK4 expression and phosphorylation of PDH.[22]

Our results illustrate a greater susceptibility to myocardial I/R injury in pressure-overloaded hearts, a relatively common clinical scenario as hypertension and coronary disease often co-exist and are common causes of heart failure.[1–3,28,29] The rate of glycolysis in response to pressure-overload was not as dramatically decreased as the rate of glucose oxidation, leading to a greater mismatch between rates of glycolysis and glucose oxidation. This uncoupling between glycolysis and glucose oxidation can increase the generation of cytosolic H^+ that accumulate during ischaemia. Efflux of protons results in intracellular Na^+ overload that triggers reverse mode Na^+/Ca^{2+} exchange and Ca^{2+} overload during reperfusion,[4,34–36] which likely contributed to the poor performance of the pressure-overload hearts in response to I/R injury. The reduction in the glycogen content in pressure-overload hearts also likely contributed to the increase in susceptibility to I/R injury.[37]

While reduced carbohydrate oxidation is expected to lead to a compensatory increase in fatty acid oxidation (based on the principles of the Randle Cycle), we also detected substantial changes in the AMPK pathway in TAC hearts, which resulted in decreased malonyl CoA levels. Increased phosphorylation of AMPK likely resulted in increased phosphorylation and inhibition of ACC, thereby reducing malonyl CoA synthesis.[4,38] Malonyl CoA, an endogenous inhibitor of carnitine palmitoyltransferase 1 (CPT1), decreases fatty acid β-oxidation.[4,39] In support of this, increased myocardial fatty acid uptake and β-oxidation during high workloads is accompanied by a decrease in myocardial malonyl CoA content in pigs[40] and rats.[41] As a result, the decreased malonyl CoA levels observed in TAC hearts may account for the switch to fatty acid oxidation in the TAC hearts compared with the sham hearts.

In this study, we describe a comprehensive assessment of changes in energy metabolic rates for glucose, lactate, fatty acids, and TG in a murine pressure-overload heart disease model. In addition to a large decrease in cardiac power, pressure-overloaded hearts also had a disproportionally large increase in oxidation of TG during reperfusion, resulting in dramatic increase in the share of acetyl CoA generated from TG oxidation. We have also shown that agonist-mediated hypertrophy and diastolic dysfunction in mice also reduces myocardial glucose and lactate oxidation with no impact on fatty acid oxidation.[22] In contrast, pressure-overload introduced by TAC in rats results in early and substantial inhibition of fatty acid oxidation (with either no change or a non-significant reduction in glucose oxidation) in association with reduced cardiac power and performance.[14,15] Similarly, in the SHR model characterized by concentric hypertrophy and diastolic dysfunction (with preserved systolic function), a preference for glucose metabolism and a shift away from predominantly fatty acid oxidative metabolism occurs.[16] *In vivo* assessments of metabolic rates in the pacing-induced heart failure in dogs also showed changes similar to humans *in vivo* data,[3,12,42] with a shift from fatty acid utilization towards glucose utilization.[10,13]

These differences between the metabolic changes in animal models of heart failure must be taken into consideration when results of gene-targeted murine models of metabolism and heart failure are studied. The differences in responses of metabolic rates to heart failure could partially be attributed to the differences in the basal substrate preferences. For example, in mouse heart, GOX is much more a contributor to energy metabolism than in rat heart, whereas FOX contribution is relatively low in mouse heart compared with rat.[14,15,22,23] Enhancing glucose oxidation may prove to be beneficial in heart failure as an attempt to use an 'oxygen-efficient' energy substrate for ATP synthesis. Dichloroacetate, a compound that enhances glucose oxidation, increases energy reserves and improves cardiac function and survival in heart failure in SHR.[43] Similarly, stimulating glucose oxidation via targeting either PDH or MCD decreases an infarct size in murine models, validating the concept that optimizing myocardial metabolism may be an effective therapy for ischaemic heart disease.[23,30]

Supplementary material

Supplementary material is available at *Cardiovascular Research* online.

Conflict of interest: none declared.

Funding

This work was supported by the Canadian Institute for Health Research Operating Grants (MOP-10957 to A.C., MOP-10865 to G.D.L., and MOP-115200 G.Y.O.). P.Z. and J.M. are partially supported by the Alberta Transplant Institute and by Post-Doctoral Fellowship Awards from the Mazankowski Alberta Heart Institute, respectively.

References

1. McKee PA, Castelli WP, McNamara PM, Kannel WB. The natural history of congestive heart failure: the Framingham study. *N Engl J Med* 1971;**285**:1441–1446.
2. McMurray JJ, Pfeffer MA. Heart failure. *Lancet* 2005;**365**:1877–1889.
3. Neubauer S. The failing heart – an engine out of fuel. *N Engl J Med* 2007;**356**:1140–1151.
4. Lopaschuk GD, Ussher JR, Folmes CD, Jaswal JS, Stanley WC. Myocardial fatty acid metabolism in health and disease. *Physiol Rev* 2010;**90**:207–258.
5. Hunter JJ, Chien KR. Signaling pathways for cardiac hypertrophy and failure. *N Engl J Med* 1999;**341**:1276–1283.
6. Chien KR, Ross J Jr, Hoshijima M. Calcium and heart failure: the cycle game. *Nat Med* 2003;**9**:508–509.
7. Conway MA, Allis J, Ouwerkerk R, Niioka T, Rajagopalan B, Radda GK. Detection of low phosphocreatine to ATP ratio in failing hypertrophied human myocardium by ^{31}P magnetic resonance spectroscopy. *Lancet* 1991;**338**:973–976.
8. Beer M, Seyfarth T, Sandstede J, Landschutz W, Lipke C, Kostler H *et al.* Absolute concentrations of high-energy phosphate metabolites in normal, hypertrophied, and failing human myocardium measured noninvasively with ^{31}P-SLOOP magnetic resonance spectroscopy. *J Am Coll Cardiol* 2002;**40**:1267–1274.
9. Acampa W, Petretta M, Spinelli L, Salvatore M, Cuocolo A. Survival benefit after revascularization is independent of left ventricular ejection fraction improvement in patients with previous myocardial infarction and viable myocardium. *Eur J Nucl Med Mol Imaging* 2005;**32**:430–437.
10. Tuunanen H, Engblom E, Naum A, Scheinin M, Nagren K, Airaksinen J *et al.* Decreased myocardial free fatty acid uptake in patients with idiopathic dilated cardiomyopathy:

evidence of relationship with insulin resistance and left ventricular dysfunction. *J Card Fail* 2006;**12**:644–652.
11. Neglia D, De Caterina A, Marraccini P, Natali A, Ciardetti M, Vecoli C *et al*. Impaired myocardial metabolic reserve and substrate selection flexibility during stress in patients with idiopathic dilated cardiomyopathy. *Am J Physiol Heart Circ Physiol* 2007; **293**:H3270–3278.
12. Nagoshi T, Yoshimura M, Rosano GM, Lopaschuk GD, Mochizuki S. Optimization of cardiac metabolism in heart failure. *Curr Pharm Des* 2011;**17**:3846–3853.
13. Osorio JC, Stanley WC, Linke A, Castellari M, Diep QN, Panchal AR *et al*. Impaired myocardial fatty acid oxidation and reduced protein expression of retinoid X receptor-α in pacing-induced heart failure. *Circulation* 2002;**106**:606–612.
14. Pound KM, Sorokina N, Ballal K, Berkich DA, Fasano M, Lanoue KF *et al*. Substrate-enzyme competition attenuates upregulated anaplerotic flux through malic enzyme in hypertrophied rat heart and restores triacylglyceride content: attenuating upregulated anaplerosis in hypertrophy. *Circ Res* 2009;**104**:805–812.
15. Doenst T, Pytel G, Schrepper A, Amorim P, Farber G, Shingu Y *et al*. Decreased rates of substrate oxidation ex vivo predict the onset of heart failure and contractile dysfunction in rats with pressure overload. *Cardiovasc Res* 2010;**86**:461–470.
16. Dodd MS, Ball DR, Schroeder MA, Le Page LM, Atherton HJ, Heather LC *et al*. *In vivo* alterations in cardiac metabolism and function in the spontaneously hypertensive rat heart. *Cardiovasc Res* 2012;**95**:69–76.
17. Riehle C, Wende AR, Zaha VG, Pires KM, Wayment B, Olsen C *et al*. PGC-1β deficiency accelerates the transition to heart failure in pressure overload hypertrophy. *Circ Res* 2011;**109**:783–793.
18. Kolwicz SC Jr, Olson DP, Marney LC, Garcia-Menendez L, Synovec RE, Tian R. Cardiac-specific deletion of acetyl CoA carboxylase 2 prevents metabolic remodeling during pressure-overload hypertrophy. *Circ Res* 2012;**111**:728–738.
19. Oudit GY, Kassiri Z, Zhou J, Liu QC, Liu PP, Backx PH *et al*. Loss of PTEN attenuates the development of pathological hypertrophy and heart failure in response to biomechanical stress. *Cardiovasc Res* 2008;**78**:505–514.
20. Guo D, Kassiri Z, Basu R, Chow FL, Kandalam V, Damilano F *et al*. Loss of PI3Kγ enhances cAMP-dependent MMP remodeling of the myocardial N-cadherin adhesion complexes and extracellular matrix in response to early biomechanical stress. *Circ Res* 2010;**107**:1275–1289.
21. Zhong J, Basu R, Guo D, Chow FL, Byrns S, Schuster M *et al*. Angiotensin-converting enzyme 2 suppresses pathological hypertrophy, myocardial fibrosis, and cardiac dysfunction. *Circulation* 2010;**122**:717–728.
22. Mori J, Basu R, McLean BA, Das SK, Zhang L, Patel VB *et al*. Agonist-induced hypertrophy and diastolic dysfunction is associated with selective reduction in glucose oxidation: a metabolic contribution to heart failure with normal ejection fraction. *Circ Heart Fail* 2012;**5**:493–503.
23. Ussher JR, Wang W, Gandhi M, Keung W, Samokhvalov V, Oka T *et al*. Stimulation of glucose oxidation protects against acute myocardial infarction and reperfusion injury. *Cardiovasc Res* 2012;**94**:359–369.
24. Saddik M, Lopaschuk GD. Myocardial triglyceride turnover and contribution to energy substrate utilization in isolated working rat hearts. *J Biol Chem* 1991;**266**: 8162–8170.
25. Fraser H, Lopaschuk GD, Clanachan AS. Assessment of glycogen turnover in aerobic, ischemic, and reperfused working rat hearts. *Am J Physiol* 1998;**275**:H1533–1541.
26. Ussher JR, Koves TR, Jaswal JS, Zhang L, Ilkayeva O, Dyck JR *et al*. Insulin-stimulated cardiac glucose oxidation is increased in high-fat diet-induced obese mice lacking malonyl CoA decarboxylase. *Diabetes* 2009;**58**:1766–1775.
27. Fraser H, Lopaschuk GD, Clanachan AS. Alteration of glycogen and glucose metabolism in ischaemic and post-ischaemic working rat hearts by adenosine A_1 receptor stimulation. *Br J Pharmacol* 1999;**128**:197–205.
28. Gheorghiade M, Sopko G, De Luca L, Velazquez EJ, Parker JD, Binkley PF *et al*. Navigating the crossroads of coronary artery disease and heart failure. *Circulation* 2006; **114**:1202–1213.
29. McMurray JJ, Adamopoulos S, Anker SD, Auricchio A, Bohm M, Dickstein K *et al*. ESC Guidelines for the diagnosis and treatment of acute and chronic heart failure 2012: The Task Force for the Diagnosis and Treatment of Acute and Chronic Heart Failure 2012 of the European Society of Cardiology. Developed in collaboration with the Heart Failure Association (HFA) of the ESC. *Eur Heart J* 2012;**33**: 1787–1847.
30. Ardehali H, Sabbah HN, Burke MA, Sarma S, Liu PP, Cleland JG *et al*. Targeting myocardial substrate metabolism in heart failure: potential for new therapies. *Eur J Heart Fail* 2012;**14**:120–129.
31. Paternostro G, Pagano D, Gnecchi-Ruscone T, Bonser RS, Camici PG. Insulin resistance in patients with cardiac hypertrophy. *Cardiovasc Res* 1999;**42**:246–253.
32. Hu P, Zhang D, Swenson L, Chakrabarti G, Abel ED, Litwin SE. Minimally invasive aortic banding in mice: effects of altered cardiomyocyte insulin signaling during pressure overload. *Am J Physiol Heart Circ Physiol* 2003;**285**:H1261–1269.
33. Liao R, Jain M, Cui L, D'Agostino J, Aiello F, Luptak I *et al*. Cardiac-specific overexpression of GLUT1 prevents the development of heart failure attributable to pressure overload in mice. *Circulation* 2002;**106**:2125–2131.
34. Weber CR, Piacentino V, Houser SR, Bers DM. Dynamic regulation of sodium/calcium exchange function in human heart failure. *Circulation* 2003;**108**:2224–2229.
35. Stanley WC, Recchia FA, Lopaschuk GD. Myocardial substrate metabolism in the normal and failing heart. *Physiol Rev* 2005;**85**:1093–1129.
36. Nakamura TY, Iwata Y, Arai Y, Komamura K, Wakabayashi S. Activation of Na^+/H^+ exchanger 1 is sufficient to generate Ca^{2+} signals that induce cardiac hypertrophy and heart failure. *Circ Res* 2008;**103**:891–899.
37. Omar MA, Wang L, Clanachan AS. Cardioprotection by GSK-3 inhibition: role of enhanced glycogen synthesis and attenuation of calcium overload. *Cardiovasc Res* 2010;**86**:478–486.
38. Folmes CD, Wagg CS, Shen M, Clanachan AS, Tian R, Lopaschuk GD. Suppression of 5′-AMP-activated protein kinase activity does not impair recovery of contractile function during reperfusion of ischemic hearts. *Am J Physiol Heart Circ Physiol* 2009;**297**: H313–321.
39. Ussher JR, Lopaschuk GD. The malonyl CoA axis as a potential target for treating ischaemic heart disease. *Cardiovasc Res* 2008;**79**:259–268.
40. Hall JL, Lopaschuk GD, Barr A, Bringas J, Pizzurro RD, Stanley WC. Increased cardiac fatty acid uptake with dobutamine infusion in swine is accompanied by a decrease in malonyl CoA levels. *Cardiovasc Res* 1996;**32**:879–885.
41. Goodwin GW, Taegtmeyer H. Regulation of fatty acid oxidation of the heart by MCD and ACC during contractile stimulation. *Am J Physiol* 1999;**277**:E772–777.
42. Davila-Roman VG, Vedala G, Herrero P, de las Fuentes L, Rogers JG, Kelly DP *et al*. Altered myocardial fatty acid and glucose metabolism in idiopathic dilated cardiomyopathy. *J Am Coll Cardiol* 2002;**40**:271–277.
43. Kato T, Niizuma S, Inuzuka Y, Kawashima T, Okuda J, Tamaki Y *et al*. Analysis of metabolic remodeling in compensated left ventricular hypertrophy and heart failure. *Circ Heart Fail* 2010;**3**:420–430.